Developmental Biology 358 (2011) 231–239

Contents lists available at ScienceDirect

Developmental Biology

journal homepage: www.elsevier.com/developmentalbiology

Ablation of *Tpbpa*-positive trophoblast precursors leads to defects in maternal spiral artery remodeling in the mouse placenta

Dong Hu, James C. Cross *

Department of Comparative Biology & Experimental Medicine, Faculty of Veterinary Medicine, and the Graduate Program in Biochemistry & Molecular Biology, University of Calgary, Calgary, Alberta, Canada

ARTICLE INFO

Article history:
Received for publication 18 March 2011
Revised 24 July 2011
Accepted 27 July 2011
Available online 4 August 2011

Keywords:
Cell ablation
Cre recombinase
Diphtheria toxin A
Trophoblast

ABSTRACT

The placenta is composed of multiple trophoblast cell types that have diverse endocrine, vascular and nutrient transport functions. We have developed a transgenic system to investigate the developmental and functional roles of specific cell types using conditional expression of a cytotoxin to induce cell ablation in transgenic mice. The *Tpbpa* gene is expressed in ectoplacental cone cells starting between embryonic days (E) 7.5 and 8.5, and later in the spongiotrophoblast layer of the mature placenta. *Tpbpa*-positive cells are progenitors of many trophoblast subtypes including three subtypes of trophoblast giant cells (TGCs) and glycogen trophoblast cells. We used a Cre recombinase transgene driven by the *Tpbpa* promoter to irreversibly activate a diphtheria toxin A (DTA) transgene. Cre/DTA double transgenic placentas showed dramatic reduction of *Tpbpa*-positive spongiotrophoblast cells by E10.5 and conceptuses died by ~E11.5. The number of cells associated with maternal blood spaces, spiral artery TGCs (SpA-TGCs) and canal TGCs, and glycogen trophoblast cells were reduced. The loss of these specific trophoblast subtypes, especially SpA-TGCs, was correlated with a decrease in maternal spiral artery diameters, indicating a critical role of these cells in modulating the maternal vasculature. In contrast, parietal TGCs were not significantly reduced by progenitor cell ablation, suggesting that there is compensatory growth of this population and indeed a population of *Ascl2* (*Mash2*)-positive/*Tpbpa*-negative cells was increased in the spongiotrophoblast layer in the Cre/DTA double transgenics. Our work demonstrates that the *Tpbpa*-positive lineage is essential for placental function and particularly critical for maternal vasculature remodeling.

Introduction

A key process during pregnancy is that the feto-placental unit builds an intimate relationship with the mother through alteration of the uterine environment and facilitation of maternal blood through the placenta (Cross et al., 2002). At the feto-maternal interface, maternal blood flow through the placenta increases dramatically due to not only blood vessel growth into the implantation site after uterine decidualization (angiogenesis), but also a significant vasodilation that results in increased blood flow (Cross et al., 2002). These processes are thought to be regulated by the interactions of various trophoblast cell subtypes in the fetal placenta with maternal endothelial cells and immune cells. However, the definitive function of specific trophoblast cell subtypes has not been well studied due to the lack of appropriate models. Mouse trophoblast giant cells (TGCs) and glycogen trophoblast cells are analogous to invading extravillous cytotrophoblast cells of the human placenta and invade the utero-placental spiral arteries or interstitially into the decidua, respectively, and are associated with the remodeling of the spiral arteries into dilated, inelastic tubes without maternal vasomotor control. Disturbed remodeling in humans leads to increased utero-placental vascular resistance and is commonly found associated with intrauterine growth restriction and preeclampsia (Kaufmann et al., 2003; Lyall and Belfort, 2007). Thus, understanding the role of specific trophoblast cells subtypes will provide us insights into human placenta pathologies and diseases of pregnancy.

TGCs are thought to be critical for embryo implantation, establishment of the feto-maternal interface and maternal adaptations to pregnancy based on their obvious invasive and endocrine properties. Four TGC subtypes have been reported within the mature placenta: parietal TGCs that line the implantation site (P-TGCs), those found invading the maternal spiral arteries (SpA-TGCs), TGCs within the maternal blood canals (C-TGCs) that connect the spiral arteries with the labyrinth layer, and TGCs found within the sinusoidal spaces of the labyrinth (S-TGCs) (Simmons et al., 2007). Their distinct locations and expression of prolactin-like protein hormones (Simmons et al., 2008) suggest that they play distinct roles at the feto-maternal interface. Cells within the ectoplacental cone and later the spongiotrophoblast layer are recognized as being progenitors of TGCs and express the spongiotrophoblast-specific gene *4311*/*Tpbpa* (Carney et al., 1993; Lescisin et al., 1988). The lineage relationship between *Tpbpa*-positive

* Corresponding author. Fax: +1 403 270 0737.
E-mail address: jcross@ucalgary.ca (J.C. Cross).

0012-1606/$ – see front matter © 2011 Elsevier Inc. All rights reserved.
doi:10.1016/j.ydbio.2011.07.036

spongiotrophoblast cells and the TGC subtypes was shown using lineage tracing in which *Tpbpa-Cre* transgenic mice were crossed with mice carrying a Cre recombinase-activated reporter gene. *Tpbpa*-positive cells were found to give rise to all SpA-TGCs, as well as ~50% of C-TGCs and P-TGCs, but none of the S-TGCs (Simmons et al., 2007). To investigate the function of cells that are derived from *Tpbpa*-positive cells, and in particular SpA-TGCs, we crossed the *Tpbpa-Cre* mice with mice carrying a Cre-activated diphtheria toxin A (DTA) transgene. As a result, we were able to specifically ablate the *Tpbpa*-positive lineage and assess the consequences for establishment of the feto-maternal interface.

Materials and methods

Animals

Tpbpa-Cre transgenic mice (Simmons et al., 2007) were bred and maintained on a C57BL6 background. Line 5 *Tpbpa-Cre-GFP* mice are used for our studies since the temporal and spatial expression of GFP in this line is similar to endogenous *Tpbpa* expression (Calzonetti et al., 1995; Simmons et al., 2007). *ROSA26-eGFP-DTA* transgenic mice (Ivanova et al., 2005) were obtained from the Jackson Laboratory (Bar Harbor, ME, USA Strain Name: STOCK *Gt(ROSA)26Sor*$^{tm1(DTA)Jpmb}$/J Stock Number: 006331). For cell ablation, *ROSA26-eGFP-DTA* homozygous female mice (*DTA/DTA*) were crossed with *Tpbpa-Cre* male mice. Of their progeny, half were *DTA/+;Tpbpa-Cre* double transgenic that undergo Cre-activated cell ablation and half are single transgenic mice (*DTA/+*). All animal procedures in this study were carried out in accordance with the guidelines of the Canadian Council on Animal Care and the University of Calgary Animal Welfare Committee (Protocol No. M06045).

Genotyping

Genotypes of the embryos and adult animals were determined by polymerase chain reaction (PCR). Genomic DNA was isolated from yolk sac or ear notches of embryos or adult mice. Primers (transgenic primer: 5′-gcg aag agt ttg tcc tca acc-3′, common primer: 5′-aaa gtc gct ctg agt tgt tat-3′, wild type reverse primer: 5′-gga ggg gga gaa atg gat atg-3′) were used for detecting *DTA* transgenic and wildtype alleles. Primers (forward primer: 5′-tcc agt gac agt ctt gat cct taa t-3′, reverse primer: 5′-aaa ttt tgg tgt acg gtc agt aaa t-3′) were used for detecting the *Tpbpa-Cre* transgene.

Tissue preparation, H&E staining and immunohistochemistry

Placentas and embryos were dissected and harvested from timed matings (E9.5, 10.5, 11.5 and 12.5) and fixed overnight in 4% paraformaldehyde in phosphate-buffered saline (PBS). Tissues were then rinsed in PBS for three times. For paraffin embedding, tissues were dehydrated through a graded ethanol series and embedded in paraffin wax. Paraffin blocks were stored and cut at room temperature. For frozen histological sections, tissues were incubated in 10% and 25% sucrose in PBS for 2 overnights, embedded in OCT at 4 °C for 2 h, and frozen in ethanol bath with dry ice. OCT blocks were then stored at −70 °C and cut at −20 °C. Histological sections were stained with Hematoxylin (Sigma Gill No.2 GHS232) and Eosin.

To investigate the localization and expression pattern of perforin in the implantation sites, the hydrated paraffin sections were incubated with 1:200 rat anti-mouse perforin monoclonal antibody (Abcam Ab16074) overnight at 4 °C after heat-mediated antigen retrieval. Detection of the primary antibody was carried out using a peroxidase-conjugated donkey anti-rat IgG (H+L) secondary antibody 1:300 (Jackson ImmunoResearch, 712-035-150). After the detection of peroxidase activity using diaminobenzidine (DAB), the sections were briefly counterstained with hematoxylin and mounted. Interferon-γ expression was detected on the acetone-fixed frozen sections using 1:200 rabbit an anti-mouse interferon-γ polyclonal antibody (Abbiotec 250708).

RNA in situ hybridization on tissue sections

RNA in situ hybridization on paraffin sections was carried out as previously described (Simmons et al., 2007). Conceptuses were dissected out of the uterus at E9.5, 10.5, 11.5 and 12.5 (E0.5 is defined as noon of the day on which vaginal plugging was detected). In situ probes used included: *Prl3d1/Pl1*, *Prl3b1/Pl2*, *Prl2c2/Plf*, *Prl4a1/Plpa*, *Pcdh12*, *Pecam1*, *Tpbpa* (Simmons et al., 2008) and *Ascl2/Mash2* (Scott et al., 2000). Digoxigenin-labeled probes were prepared by using digoxigenin labeling mix (Boehringer Mannheim) and detected by using an anti-digoxigenin–alkaline phosphatase conjugate (Boehringer Mannheim).

For double in situ hybridization experiments, the same protocol was carried out on cryo-sections with minor modifications. Detailed procedures were described before (Simmons et al., 2007). Probes labeled with fluorescein as well as digoxigenin according to the manufacturer's instructions and added to the hybridization mix. After the digoxigenin probe was detected with NBT/BCIP, the enzyme was inactivated with heating to 65 °C for 30 min in 1× MABT, followed by 30 min incubation in 0.1 M glycine pH2.2, blocked for 1 h in blocking solution and incubated overnight at 4 °C with anti-fluorescein antibody (Roche, 1:2500). Fluorescein probes were detected by incubation with INT/BCIP (Roche) until a brown precipitate formed. Reactions were stopped in PBS, counterstained with nuclear fast red, and mounted under 50% glycerol/PBS for microscopy.

Phospho-histone H3 immunohistochemistry following in situ hybridization

OCT embedded cryo-sections were processed initially as for regular in situ hybridization. After the digoxigenin probe was detected with NBT/BCIP, sections were washed in PBS and blocked with normal donkey serum from the host species of the secondary antibody for 1 h. Sections were incubated with anti-phospho-histone H3 (1:200; Upstate 06-570) overnight at 4 °C and then incubated with 1:300 Donkey anti-rabbit HRP conjugated secondary antibody (NA934V, GE healthcare) for 1 h. Each step was separated by careful washings in PBS. Colorimetric staining was done with diaminobenzidine.

TUNEL

The DeadEnd Colorimetric TUNEL system was used to assess apoptosis (Promega, G7130 Madison, USA) according to manufacturer's instructions. Paraffin sections were de-paraffinized in fresh xylene, rehydrated and incubated with 20 μg/ml of proteinase K for 15 min and rinsed in PBS. The sections were incubated with equilibration buffer for 5–10 min and then with rTdT (Terminal Deoxynucleotidyl Transferase, Recombinant) reaction mix including rTdT enzyme and biotinylated nucleotide mix in a humidified atmosphere at 37 °C for 60 min. They were subsequently washed by immersing the slides in 2× SSC for at room temperature for 15 min. The endogenous peroxidase activity was blocked with 0.3% hydrogen peroxide. The sections were then incubated with Streptavidin HRP for 30 min. Each step was separated by careful washings in PBS. Staining was done with diaminobenzidine.

Quantitative analysis of P-TGCs, SpA-TGC lined spiral arteries, spiral artery diameter and maternal blood space

For quantitative analysis of *Prl3d1/Pl1*-positive P-TGCs, 8 different placentas each from E10.5 control (*DTA/+*) conceptuses and *DTA/+; Tpbpa-Cre* conceptuses respectively were studied. Four sagittal, non-adjacent sections with even distance apart at the center of the placenta were stained with *Prl3d1/Pl1* and used for measurement of *Prl3d1/Pl1*-

Table 1
Genotyping and viability of offspring from *DTA/DTA* and *Tpbpa-Cre/+* mice crosses.

	Genotypes					Total
	DTA/+		*DTA/+;Tpbpa-Cre*		RS[a]	
	Dead embryos	Viable embryos	Dead embryos	Viable embryos		
E9.5	0	21	0	27	3	51
E10.5	0	21	6	21	2	50
E11.5	0	22	18	0	1	41
E12.5	0	16	26	0	4	46

[a] Very early resorption sites that the genotype cannot be determined.

positive cell number per section and area. The ImageJ manual counting and area measurement tool was used for the analysis.

For quantitative analysis of spiral arteries lined by *Prl2c2/Plf*-positive SpA-TGCs and spiral artery diameter, serial transverse sections of E10.5 conceptuses were prepared and subjected to in situ hybridization with probes for *Prl3d1/Pl1* and *Prl2c2/Plf* for TGCs, and *Pecam1* for endothelial cells. To provide a reference point for the extent of trophoblast invasion in different samples, histological sections just above the layer of P-TGCs surrounding the implantation site, with minimal *Prl3d1/Pl1* staining at the center, were defined as the "0 μm" starting point for SpA-TGC invasion (Fig. 3A). The number of sections above that point and their thickness (8 μm) was used to estimate the depth of invasion. For example, the sections 160 μm farther back into the decidua were defined as "160 μm". The number of spiral arteries lined by *Prl2c2/Plf*-positive cells at 0 μm and 160 μm was counted in 4 different normal (*DTA/+*) and 5 different *DTA/+;Tpbpa-Cre* conceptuses. For measuring spiral artery diameter, the number of spiral arteries in normal placenta was first determined by measuring number of lumens lined by *Prl2c2/Plf*-positive cells. The diameters of spiral arteries were then determined by measuring the minimum lumen diameter of the five largest arteries labeled by *Pecam1*-positive cells within the central half of the transverse sections. This distinguished the arteries from the maternal veins which are more peripherally located (Adamson et al., 2002).

For quantitative analysis of the maternal blood space in the labyrinth, paraffin sections of E10.5 conceptuses were stained with hematoxylin and eosin. For each conceptus at E10.5, three different pictures on the labyrinth of the placenta were taken. The maternal blood space was identified by the presence of non-nucleated maternal red blood cells within it. The area fraction of maternal blood space was estimated by ImageJ as the proportion of the total labyrinth area occupied by maternal blood space.

Results

DTA/+;Tpbpa-Cre double transgenic conceptuses die at mid-gestation

To induce cell type specific ablation of the *Tpbpa*-positive trophoblast lineage, we crossed *Tpbpa-Cre* transgenics (Simmons

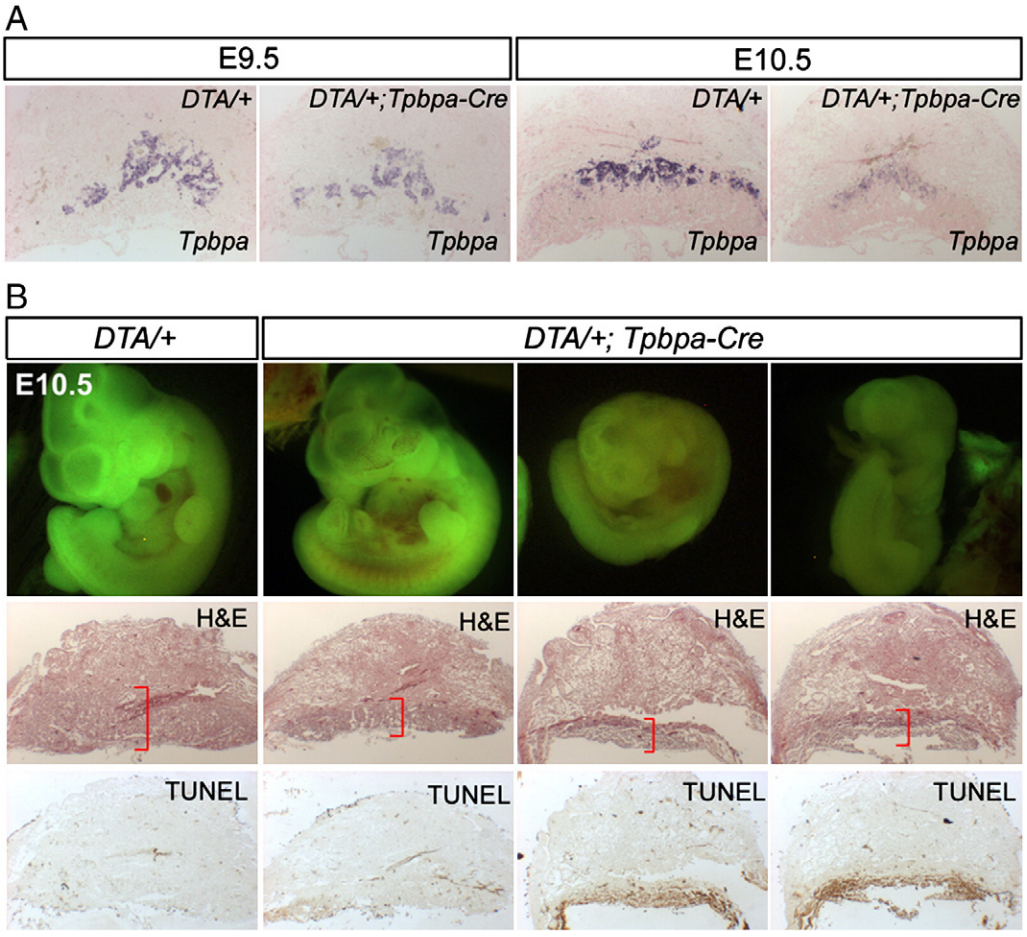

Fig. 1. *Tpbpa*-positive lineage ablation is underway by E10.5 and results in embryonic lethality associated with apoptosis within the placenta. (A) *Tpbpa* mRNA expression in control (*DTA/+*) and *DTA/+;Tpbpa-Cre* double transgenic placentas. Note that expression is not strikingly reduced until E10.5, indicating *Tpbpa*-positive lineage ablation by Cre activated DTA system is underway at around E10.5. (B) Whole mount view of fetuses (top row) and histological sections of placentas stained with H&E or TUNEL for cell death. Note that *DTA/+;Tpbpa-Cre* double transgenic mice start to die at around E10.5, with some variability in phenotype, which is associated with reduced size as shown by H&E staining and increased apoptosis as shown by TUNEL staining of the placenta.

et al., 2007) with mice carrying a conditionally-activated DTA gene (Ivanova et al., 2005). This approach allows the conditional expression of DTA upon Cre-mediated excision of a floxed region containing transcriptional termination sequences, resulting in death of ectoplacental cone/spongiotrophoblast cells that express *Tpbpa-Cre*. Characterization of progeny from E9.5 to 12.5 indicated that *DTA/+;Tpbpa-Cre* conceptuses started to die by ~E10.5 and none of them survived beyond E11.5, whereas *DTA/+* mice were fully viable (Table 1 and Fig. 1B). To assess when the cell ablation starts, we examined placentas for the presence of ectoplacental cone/spongiotrophoblast cells by expression of the endogenous *Tpbpa* gene. The number of *Tpbpa*-expressing cells was dramatically reduced in the placenta by ~E10.5 (Fig. 1A). This fit with histological assessment of the placentas at E10.5 which showed that the size of *DTA/+;Tpbpa-Cre* placentas was dramatically reduced and was associated with increased apoptosis of cells as shown by TUNEL staining (Fig. 1B). Interestingly, TUNEL-positive cells were observed not only in the spongiotrophoblast but also the labyrinth layer. Since *Tpbpa*-positive cells do not contribute to the labyrinth (Simmons et al., 2007), the latter effect is likely a secondary consequence. These data indicated that although *Tpbpa-Cre* starts to express at least as early as E8.5 (Simmons et al., 2007), cell ablation only becomes extensive around two days later. Delays in cell death after the onset of DTA expression have been reported previously (Brockschnieder et al., 2004; Ivanova et al., 2005) and presumably reflect that time is required for the toxin to accumulate and/or that trophoblast cells are somewhat resistant.

Trophoblast cell ablations in DTA/+;Tpbpa-Cre conceptuses

To assess the consequences of ablating *Tpbpa*-positive cells on the trophoblast cell lineage that is normally derived from these cells, we characterized the placentas of *DTA/+;Tpbpa-Cre* and control (*DTA/+*) conceptuses using cell subtype specific markers. Glycogen trophoblast cells were identified by labeling of *Pcdh12* mRNA and were found to be reduced in E10.5 conceptuses (Fig. 2A, data not shown). Staining of SpA-TGCs by *Prl2c2/Plf* (Proliferin) demonstrated that while SpA-TGCs were present lining the spiral arteries in control conceptuses, very few *Prl2c2/Plf*-positive cells were detected invading into the decidua of *DTA/+;Tpbpa-Cre* conceptuses (Fig. 2A). Staining of C-TGCs by *Prl2c2/Plf* also showed that *Prl2c2/Plf*-positive cells were far fewer in the *DTA/+;Tpbpa-Cre* conceptuses compared to controls (Fig. 2A). In contrast, staining of P-TGCs by labeling *Prl3d1/Pl1* (Placental lactogen 1) was not significantly different (Fig. 2A). Quantitative analysis demonstrated that *Prl3d1/Pl1*-positive cell number and size was not significantly different in *DTA/+;Tpbpa-Cre* compared to control conceptuses at E10.5 (Figs. 2B and C).

Reduction in spiral artery lumen diameter and decreased maternal blood in the labyrinth

SpA-TGCs are thought to increase maternal blood flow to the implantation site by invading into the lumen of spiral arteries (Adamson et al., 2002). Staining of *Prl2c2/Plf* on transverse section

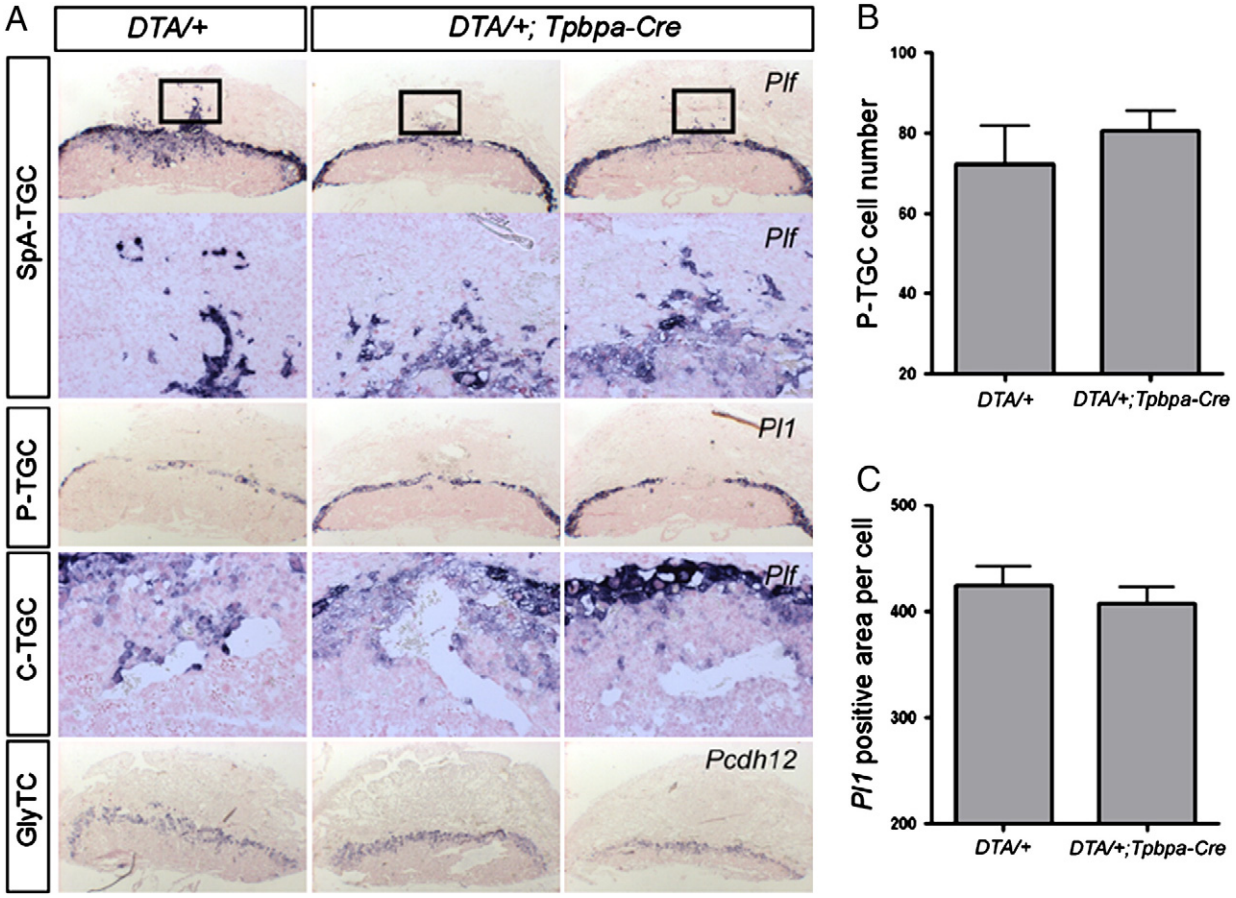

Fig. 2. Consequences of trophoblast cell type loss after *Tpbpa* positive lineage ablation at E10.5. (A) In situ hybridization using marker genes for various TGC subtypes and glycogen trophoblast cells (GlyTC). *Tpbpa*-positive cell ablation results in reduction of spiral artery associated TGC (SpA-TGCs), canal TGCs (C-TGCs) and glycogen trophoblast cells (GlyTCs) but not parietal TGCs (P-TGCs) as shown by staining of their markers at E10.5. (B) P-TGC number per section. Note that it is not significantly reduced ($P>0.05$). (C) P-TGC size (arbitrary units) is not significantly reduced ($P>0.05$).

of the implantation sites (decidua plus placenta) showed that in E10.5 control conceptuses, there were 5.5 ± 0.65 spiral arteries containing *Prl2c2/Plf*-positive SpA-TGCs at the point that the arteries converge at the P-TGC layer (Fig. 3A). In contrast, only 2.6 ± 0.60 ($P<0.05$) spiral arteries containing SpA-TGCs were detected in *DTA/+;Tpbpa-Cre* conceptuses at the corresponding plane of section. In addition, whereas SpA-TGCs were readily detected in control placentas 160 μm upstream as a result of endovascular invasion, almost no *Prl2c2/Plf*-positive cells were detected upstream in the *DTA/+;Tpbpa-Cre* placentas. Quantitative analysis also showed that spiral artery diameter was less than half in *DTA/+;Tpbpa-Cre* conceptuses compared to controls ($P<0.05$) (Fig. 3B). To assess whether the reduced spiral artery diameter affected overall maternal blood delivery into the placenta, we estimated the volume fraction of maternal blood space (MBS) within the labyrinth by measuring the proportion of the labyrinth cross-sectional area occupied by maternal blood spaces and found that it was reduced by ~50% (Fig. 3C).

While our data clearly implicated the *Tpbpa*-lineage in the normal dilatation of spiral arteries during pregnancy, uterine natural killer (uNK) cells from the mother are also thought to play a role (Ashkar and Croy, 2001). TGCs may regulate uNK cell activity resulting from the production of the prolactin-like protein hormone PLP-A (Ain et al., 2003). The *Prl4a1/Plpa* gene is expressed by the P-TGC, SpA-TGC and C-TGCs in wildtype placentas (Simmons et al., 2008) and its expression was significantly reduced in *DTA/+;Tpbpa-Cre* conceptuses (Fig. 4). However, staining of uNK cells with an antibody against perforin (pore-forming protein) showed that the number and localization of differentiated uNK cells was not obviously different (Fig. 4). We also used immunohistochemistry to assess the expression of interferon-γ, which is produced by uNK cells and is implicated in spiral artery remodeling (Ashkar et al., 2000), but found no obvious difference (Fig. 4). These data suggest that the reduced diameter of spiral arteries is more likely due to differences in trophoblast cell function directly than to the effects on uNK cell localization or function. However, due to the nature of the method we used for detecting interferon-γ, we cannot preclude the possibility that interferon-γ released from cells might be different.

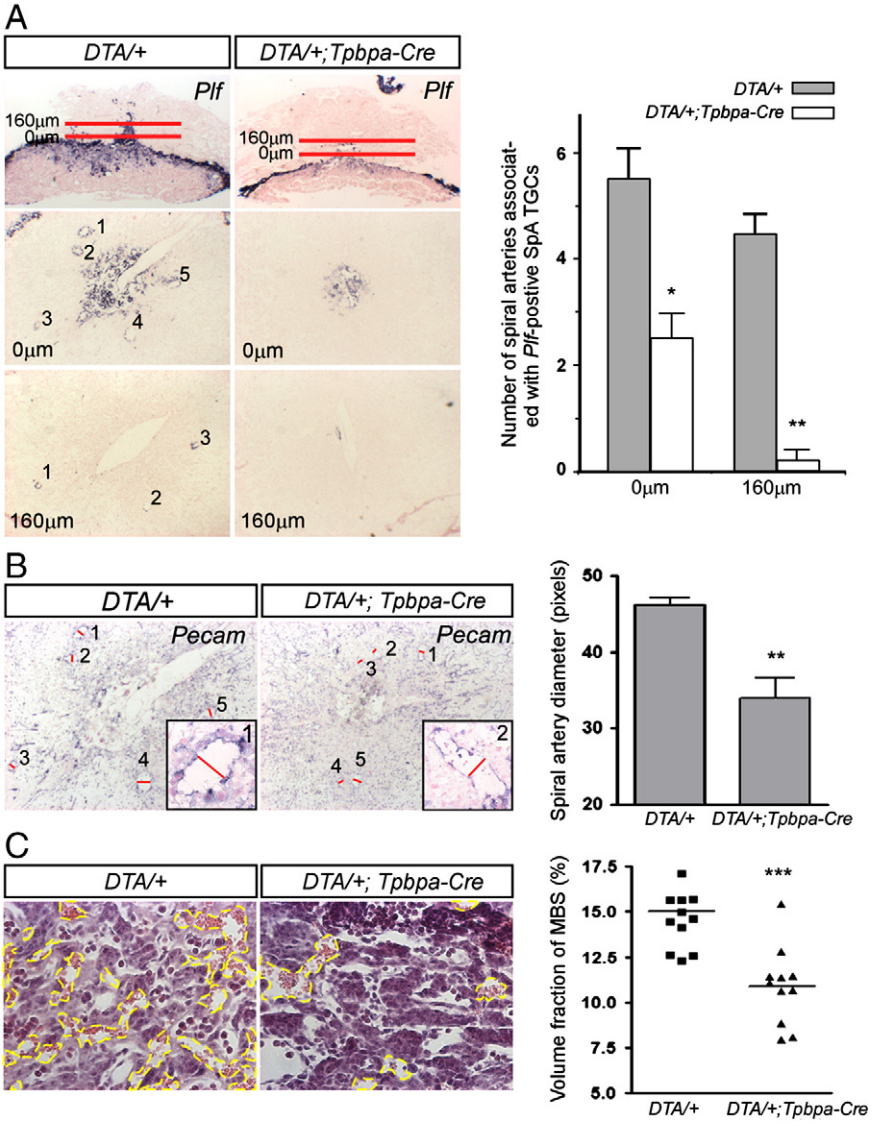

Fig. 3. Reduction of SpA-TGCs invasion is associated with reduced dilation of spiral arteries and is associated with decreased maternal blood in the labyrinth. (A) Assessment of the number of spiral arteries containing *Prl2c2/Plf*-positive SpA-TGCs and the depth of their invasion upstream in the spiral artery. *Tpbpa*-positive cell ablation results in reduction of spiral arteries lined by SpA-TGC at E10.5. (B) Spiral artery lumen diameter. Note that it is reduced in *DTA/+;Tpbpa-Cre* conceptuses at E10.5 ($P<0.05$). (C) Proportion of the labyrinth cross-sectional area that is occupied by maternal blood space (MBS). Yellow dashed line outlines the maternal blood space. Note that it is significantly reduced in *DTA/+;Tpbpa-Cre* conceptuses at E10.5 ($P<0.05$).

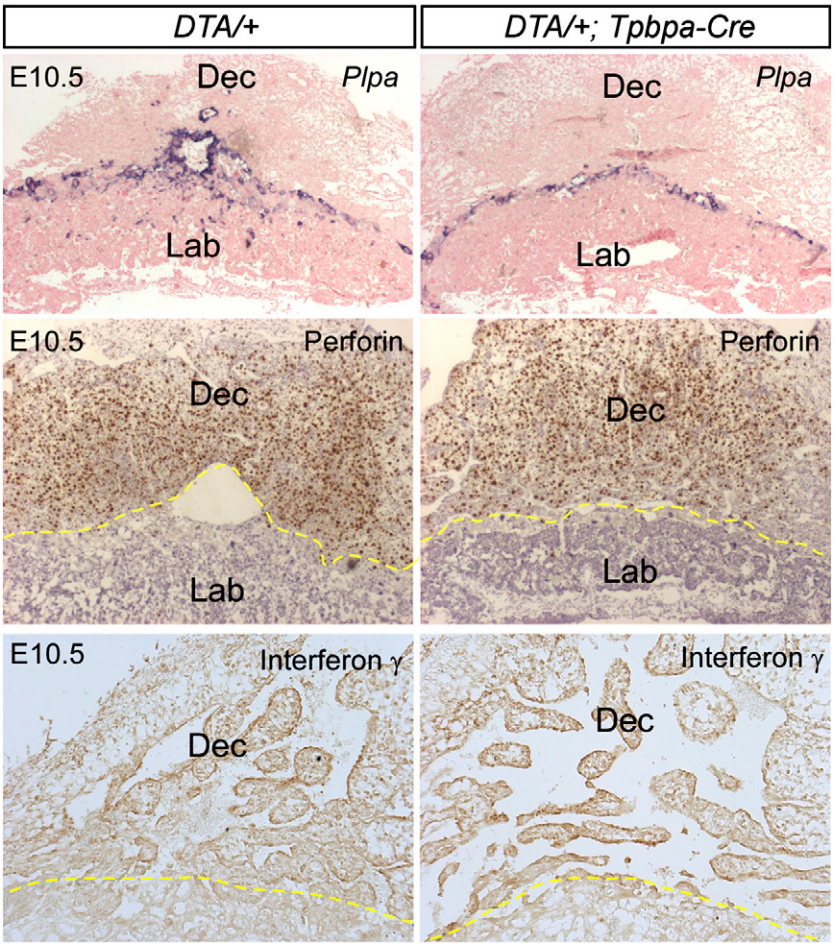

Fig. 4. *Prl4a1*/*Plpa* expression is reduced in *DTA/+;Tpbpa-Cre* conceptuses with no change in perforin-positive uNK cells distribution. *Tpbpa*-positive cell ablation results in reduction of *Prl4a1*/*Plpa*-expressing cells at E10.5. In contrast, that the number and distribution of mature uNK cells was not obviously different as shown by perforin protein staining. The interferon γ expression in implantation sites by immunohistochemistry staining did not show significant changes after *Tpbpa*-positive cell ablation. The yellow dashed line separates the decidua and implantation site. Dec, Decidua; Lab, Labyrinth.

Increased proliferation of Tpbpa-negative/Ascl2-positive spongiotrophoblast cells

In wildtype placentas, P-TGCs are derived equally from *Tpbpa*-positive and *Tpbpa*-negative precursors (Simmons et al., 2007). The finding that P-TGC cell number was not reduced in *DTA/+;Tpbpa-Cre* conceptuses at E10.5 (Fig. 2) suggested that some *Tpbpa*-negative cells can compensate for the loss of P-TGCs that normally would have been derived from the *Tpbpa*-positive lineage. Even before expression of *Tpbpa*, ectoplacental cone/spongiotrophoblast cells express *Ascl2* (previously named *Mash2*), which encodes for a basic helix–loop–helix transcription factor that is essential for spongiotrophoblast layer maintenance (Tanaka et al., 1997). Using double in situ hybridization in wildtype placentas, we found that expression of *Tpbpa* and *Ascl2* only partially overlaps within the spongiotrophoblast and that *Tpbpa*-negative/*Ascl2*-positive cells were readily detected (Fig. 5A). The number of *Tpbpa*-negative/*Ascl2*-positive cells was dramatically increased within the spongiotrophoblast layer of *DTA/+;Tpbpa-Cre* conceptuses (Fig. 5A) compared to controls. Co-staining for the mitotic marker, phospho-histone 3 showed that cell proliferation was increased within the spongiotrophoblast layer at E10.5 in the *DTA/+;Tpbpa-Cre* placentas (Figs. 5B and C). Dual staining also showed that the *DTA/+;Tpbpa-Cre* placentas had a significantly higher proportion of *Ascl2*/phospho-histone H3 double positive cells (Figs. 5B and D).

Discussion

Various TGC cell subtypes have been characterized in the placenta (Simmons et al., 2007). However, the function of these various subtypes has only been speculated and has never been directly demonstrated. Here we used a Cre activated DTA transgenic system to ablate TGC subtypes and glycogen trophoblast cells that are derived from *Tpbpa*-positive precursors. We found that *Tpbpa*-positive cell lineage is critical for remodeling spiral arteries during pregnancy and revealed an unexpected role of *Tpbpa*-negative/*Ascl2*-positive cells in being able to compensate for P-TGC cell loss.

Ablation of Tpbpa-positive cells is associated with maternal vascular changes

During rodent pregnancy, the feto-placental unit builds connections with the mother through remodeling of maternal vasculature. The process is thought to be coordinated by SpA-TGCs and uNK cells (Cross et al., 2002). Glycogen trophoblast cells also invade into the uterus but do so interstitially and only after E12.5 and not in direct association with the spiral arteries (Adamson et al., 2002). It has been suggested that MMP-9 expressed by glycogen trophoblast cells may play a role in the degradation of ECM surrounding the spiral arteries, therefore contribute to spiral artery dilation and increased maternal blood flow (Coan et al., 2006). However, glycogen trophoblast cells

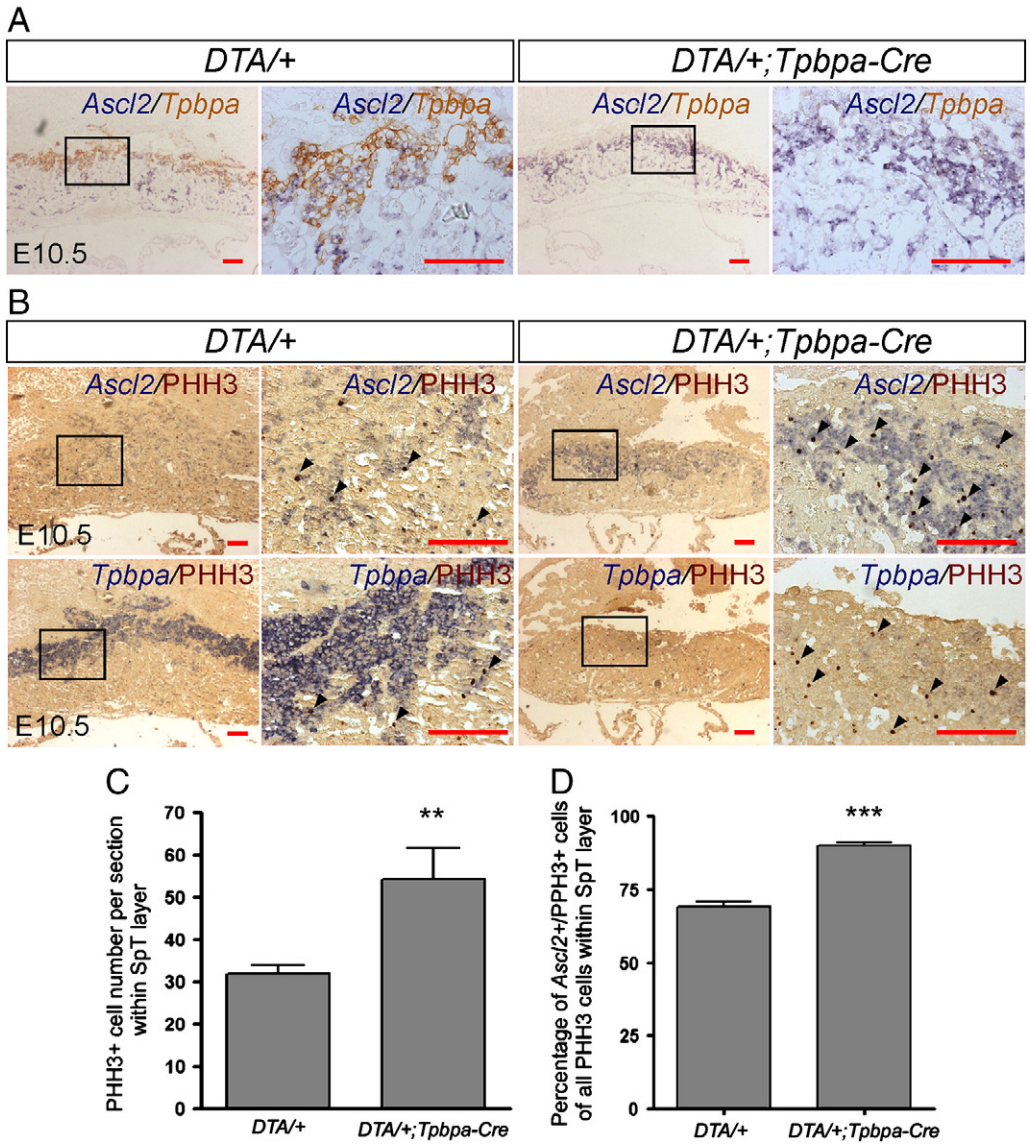

Fig. 5. *Ascl2*-positive/*Tpbpa*-negative cell number increases within spongiotrophoblast layer with elevated proliferation in *DTA/+;Tpbpa-Cre* mice. (A) Dual color in situ hybridization for *Ascl2* and *Tpbpa* mRNA expression. Note that they overlap within the spongiotrophoblast layer and *Ascl2*-positive/*Tpbpa*-negative cells increase in spongiotrophoblast layer in the *DTA/+;Tpbpa-Cre* mice at E10.5. (B) Dual staining for proliferating cells (phospho-histone 3 positive). More *Ascl2*-positive/phospho-histone 3-positive (*Ascl2+*/PHH3+) cells rather than *Tpbpa*-positive/phospho-histone 3 positive (*Tpbpa+*/PHH3+) cells are present within spongiotrophoblast layer in *DTA/+;Tpbpa-Cre* conceptuses. Arrowheads, PHH3+ cells. (C) Quantitation of proliferating cells within the spongiotrophoblast (SpT) layer. PHH3+ cell number increases significantly within the spongiotrophoblast layer in *DTA/+;Tpbpa-Cre* mice ($P<0.05$). (D) Percentage of *Ascl2+* cells within the PHH3+ cell population in SpT layer in *DTA/+;Tpbpa-Cre* conceptuses increases significantly ($P<0.05$).

invade and express MMP-9 after E12.5 (Coan et al., 2006), well after our mice have already shown the spiral artery phenotype (E10.5). This evidence likely excludes the possibility that glycogen trophoblast cells facilitate spiral artery remodeling and dilation, at least during early and mid-gestation. C-TGCs line the maternal blood canals that deliver blood from the spiral arteries into the labyrinth layer of the placenta (Adamson et al., 2002). Due to their location, C-TGCs do not immediately regulate spiral artery remodeling, but they are very likely to influence delivery of maternal blood into the labyrinth and loss of C-TGCs in the double transgenic conceptuses may contribute to reduction of maternal blood delivery. While the role of uNK cells has been established by examining the phenotype of NK deficient mice (Ashkar and Croy, 2001), the exact roles of the SpA-TGCs and how trophoblast cells interact with uNK cells are not known. One of the hormones produced by TGCs (PLP-A) has been shown to regulate uNK cell activity in vitro (Muller et al., 1999), though *Prl4a1*/*Plpa*-deficient mice do not show obvious uNK cell changes in localization as shown by perforin staining (Ain et al., 2004).

Though our current transgenic model ablates the entire lineage derived from *Tpbpa*-positive precursors, based on the timing of the phenotype, we believe that the spiral artery remodeling phenotype reflects the function of SpA-TGCs. Our previous work has shown that all of SpA-TGCs are derived from *Tpbpa*-positive precursors (Simmons et al., 2007). Thus, by breeding the *Tpbpa-Cre* mice with DTA conditional transgenic mice we were able to delete SpA-TGCs and examine the effect on pregnancy outcome. We found that the spiral arteries in the *DTA+/Tpbpa-Cre* mice were invaded by significantly fewer SpA-TGCs (*Prl2c2*/*Plf* positive), and this was associated with reduced diameters of the spiral arteries. Since SpA-TGCs are the only trophoblast cell type that is in direct contact with spiral arteries and the only trophoblast cell subtype that has invaded into the decidua by E10.5 when we observed the spiral artery phenotype (glycogen

trophoblast cells are only detected by E12.5) (Adamson et al., 2002; Simmons et al., 2007), the data strongly suggest that SpA-TGCs are required for spiral artery remodeling and lumen dilation. The significant reduction of maternal blood volume within the labyrinth is likely to be a direct consequence of the reduced spiral artery diameters.

The mechanism by which SpA-TGCs promote the dilation of spiral arteries is unknown. In humans, it has been argued that the simple act of trophoblast cell invasion into the spiral arteries replaces the endothelial and vascular smooth muscle cells leading to vessel dilation (Helwig and Le Bouteiller, 2007; Kharfi et al., 2003). However, at least in mice where spiral arteries have been studied throughout their length, the spiral arteries are dilated throughout their length despite only being invaded in the distal 20–30% (Adamson et al., 2002). The alternative hypothesis is that SpA-TGCs have paracrine effects to promote spiral artery remodeling. SpA-TGCs express various cytokines including PLF, PLF-RP, PLP-A, PLP-E and PLP-F (Simmons et al., 2008). PLF and PRP are angiogenic and anti-angiogenic factors, respectively (Jackson et al., 1994). PLP-A has a modulatory effect on uNK cells, which regulate maternal vasculature remodeling (Ain et al., 2003; Muller et al., 1999). Thus, SpA-TGCs are very likely to remodel maternal vasculature through their paracrine effects either directly on the vessels or indirectly by affecting uNK cell activity. In our *Tpbpa-Cre/DTA* model, we found dramatic decrease of PLF and PLP-A expression by SpA-TGC. We found no obvious change in the number or localization of differentiated uNK cells but there are no direct in situ assays for assessing their activity. Production of IFN-γ by uNK cells has been shown to play an important role in spiral artery remodeling in the decidua (Ashkar et al., 2000). Staining for IFN-γ expression by immunohistochemistry did not show a significant difference in the *Tpbpa-Cre/DTA* placenta. However, we cannot preclude the possibility that interferon-γ released from cell might be different in the *Tpbpa-Cre/DTA* implantation sites. Taken together our results suggest a direct paracrine role of SpA-TGCs in regulating maternal vasculature remodeling.

Our studies provide the first direct evidence showing the consequences of reduced trophoblast invasion on spiral artery remodeling and its potential effects on maternal blood delivery into the placenta. Endovascular cytotrophoblast cell invasion in the human placenta has been implicated with spiral artery remodeling but the evidence is indirect and based on the findings from cases of preeclampsia and intrauterine growth restriction of impaired trophoblast invasion (Guzin et al., 2005; Naicker et al., 2003) and increased uterine artery blood flow resistance (Matijevic and Johnston, 1999). These human data certainly fit the model but do not establish a causal relationship.

Compensation for the number of P-TGCs after precursor ablation

Surprisingly, unlike other TGCs subtypes that derived from *Tpbpa*-positive precursors, the number of P-TGCs did not significantly change after cell ablation at E10.5. In wildtype placentas, ~50% of P-TGCs are normally derived from *Tpbpa*-negative precursors (Simmons et al., 2007), and so it is likely that these precursors compensate for the loss of TGCs derived from the *Tpbpa*-positive cells. This implies that other cells somehow sense the number of P-TGCs and can adapt if the number is reduced. A plausible explanation is suggested by the finding that P-TGCs express the growth factor Activin, which has paracrine effects to suppress further TGC differentiation (Natale et al., 2009). To understand what might be the source of *Tpbpa*-negative cells, we carefully examined the expression of *Ascl2*, which is expressed in and required for maintenance of spongiotrophoblast and suppression of excess P-TGC differentiation (Tanaka et al., 1997), and found that *Tpbpa*-negative/*Ascl2*-positive cells are readily detected in the placenta and that their proliferation was increased following *Tpbpa*-positive cell ablation. Collectively, the data suggest several key points concerning the cell populations marked by *Ascl2* and *Tpbpa* expression. First, *Tpbpa*-positive cells likely originate from cells that are initially *Ascl2*-positive, but then become only *Tpbpa* positive. Second, there are *Ascl2*-positive/*Tpbpa*-negative cells within spongiotrophoblast layer which became dramatically increased in the *DTA/+;Tpbpa-Cre* conceptuses and these cells are the progenitors that compensate for the number of P-TGCs. The data further suggest that increased cell proliferation of *Ascl2*-positive/*Tpbpa*-negative cells within the spongiotrophoblast layer serves as a key mechanism for P-TGCs compensation.

In summary, conditional ablation of *Tpbpa*-positive cells allowed us to delete specific trophoblast cell types and to characterize the effect on pregnancy outcome. Human preeclampsia has been associated with the failure of extravillous trophoblast cell invasion into spiral arteries and disturbance of maternal vasculature remodeling. In our mouse model, we believe that the loss of SpA-TGCs resulted in spiral arteries without TGCs invasion and significant smaller lumen. Further study of this model will permit us to understand the mechanisms by which endovascular invading trophoblast cells affect spiral artery remodeling. It should be stated that a limitation of the current model, however, is that multiple cell types are impacted by ablation of *Tpbpa*-positive precursors. A second and equally important finding from the current studies is that, at least with respect to P-TGC numbers, the placenta shows developmental plasticity such that normal number of cells can be achieved even if one type of precursor is ablated early in development.

Acknowledgments

The work was supported by grants from the Canadian Institutes of Health Research and Alberta Innovates-Health Solutions.

References

Adamson, S.L., Lu, Y., Whiteley, K.J., Holmyard, D., Hemberger, M., Pfarrer, C., Cross, J.C., 2002. Interactions between trophoblast cells and the maternal and fetal circulation in the mouse placenta. Dev. Biol. 250, 358–373.

Ain, R., Tash, J.S., Soares, M.J., 2003. Prolactin-like protein-A is a functional modulator of natural killer cells at the maternal–fetal interface. Mol. Cell. Endocrinol. 204, 65–74.

Ain, R., Dai, G., Dunmore, J.H., Godwin, A.R., Soares, M.J., 2004. A prolactin family paralog regulates reproductive adaptations to a physiological stressor. Proc. Natl. Acad. Sci. U.S.A. 101, 16543–16548.

Ashkar, A.A., Croy, B.A., 2001. Functions of uterine natural killer cells are mediated by interferon gamma production during murine pregnancy. Semin. Immunol. 13, 235–241.

Ashkar, A.A., Di Santo, J.P., Croy, B.A., 2000. Interferon gamma contributes to initiation of uterine vascular modification, decidual integrity, and uterine natural killer cell maturation during normal murine pregnancy. J. Exp. Med. 192, 259–270.

Brockschnieder, D., Lappe-Siefke, C., Goebbels, S., Boesl, M.R., Nave, K.A., Riethmacher, D., 2004. Cell depletion due to diphtheria toxin fragment A after Cre-mediated recombination. Mol. Cell. Biol. 24, 7636–7642.

Calzonetti, T., Stevenson, L., Rossant, J., 1995. A novel regulatory region is required for trophoblast-specific transcription in transgenic mice. Dev. Biol. 171, 615–626.

Carney, E.W., Prideaux, V., Lye, S.J., Rossant, J., 1993. Progressive expression of trophoblast-specific genes during formation of mouse trophoblast giant cells in vitro. Mol. Reprod. Dev. 34, 357–368.

Coan, P.M., Conroy, N., Burton, G.J., Ferguson-Smith, A.C., 2006. Origin and characteristics of glycogen cells in the developing murine placenta. Dev. Dyn. 235, 3280–3294.

Cross, J.C., Hemberger, M., Lu, Y., Nozaki, T., Whiteley, K., Masutani, M., Adamson, S.L., 2002. Trophoblast functions, angiogenesis and remodeling of the maternal vasculature in the placenta. Mol. Cell. Endocrinol. 187, 207–212.

Guzin, K., Tomruk, S., Tuncay, Y.A., Naki, M., Sezginsoy, S., Zemheri, E., Yucel, N., Kanadikirik, F., 2005. The relation of increased uterine artery blood flow resistance and impaired trophoblast invasion in pre-eclamptic pregnancies. Arch. Gynecol. Obstet. 272, 283–288.

Helwig, J.J., Le Bouteiller, P., 2007. Physiological smooth muscle cell apoptosis contributes to the uterine vascular remodeling in human early pregnancy. Circ. Res. 100, 754–756.

Ivanova, A., Signore, M., Caro, N., Greene, N.D., Copp, A.J., Martinez-Barbera, J.P., 2005. In vivo genetic ablation by Cre-mediated expression of diphtheria toxin fragment A. Genesis 43, 129–135.

Jackson, D., Volpert, O.V., Bouck, N., Linzer, D.I., 1994. Stimulation and inhibition of angiogenesis by placental proliferin and proliferin-related protein. Science 266, 1581–1584.

Kaufmann, P., Black, S., Huppertz, B., 2003. Endovascular trophoblast invasion: implications for the pathogenesis of intrauterine growth retardation and preeclampsia. Biol. Reprod. 69, 1–7.

Kharfi, A., Giguere, Y., Sapin, V., Masse, J., Dastugue, B., Forest, J.C., 2003. Trophoblastic remodeling in normal and preeclamptic pregnancies: implication of cytokines. Clin. Biochem. 36, 323–331.

Lescisin, K.R., Varmuza, S., Rossant, J., 1988. Isolation and characterization of a novel trophoblast-specific cDNA in the mouse. Genes Dev. 2, 1639–1646.

Lyall, F., Belfort, M.A., 2007. Pre-eclampsia: Etiology and Clinical Practice. Cambridge University Press, Cambridge; New York.

Matijevic, R., Johnston, T., 1999. In vivo assessment of failed trophoblastic invasion of the spiral arteries in pre-eclampsia. Br. J. Obstet. Gynaecol. 106, 78–82.

Muller, H., Liu, B., Croy, B.A., Head, J.R., Hunt, J.S., Dai, G., Soares, M.J., 1999. Uterine natural killer cells are targets for a trophoblast cell-specific cytokine, prolactin-like protein A. Endocrinology 140, 2711–2720.

Naicker, T., Khedun, S.M., Moodley, J., Pijnenborg, R., 2003. Quantitative analysis of trophoblast invasion in preeclampsia. Acta Obstet. Gynecol. Scand. 82, 722–729.

Natale, D.R., Hemberger, M., Hughes, M., Cross, J.C., 2009. Activin promotes differentiation of cultured mouse trophoblast stem cells towards a labyrinth cell fate. Dev. Biol. 335, 120–131.

Scott, I.C., Anson-Cartwright, L., Riley, P., Reda, D., Cross, J.C., 2000. The HAND1 basic helix–loop–helix transcription factor regulates trophoblast differentiation via multiple mechanisms. Mol. Cell. Biol. 20, 530–541.

Simmons, D.G., Fortier, A.L., Cross, J.C., 2007. Diverse subtypes and developmental origins of trophoblast giant cells in the mouse placenta. Dev. Biol. 304, 567–578.

Simmons, D.G., Rawn, S., Davies, A., Hughes, M., Cross, J.C., 2008. Spatial and temporal expression of the 23 murine Prolactin/Placental Lactogen-related genes is not associated with their position in the locus. BMC Genomics 9, 352.

Tanaka, M., Gertsenstein, M., Rossant, J., Nagy, A., 1997. Mash2 acts cell autonomously in mouse spongiotrophoblast development. Dev. Biol. 190, 55–65.